Probing the shear modulus of two-dimensional multiplanar nanostructures and heterostructures

T. Mukhopadhyay[a*], A. Mahata[b], S. Adhikari[c], M. Asle Zaeem[b]

[a]*Department of Engineering Science, University of Oxford, Oxford, UK*
[b]*Department of Materials Science and Engineering, Missouri University of Science and Technology, Rolla, USA*
[c]*College of Engineering, Swansea University, Swansea, UK*

Abstract

Generalized high-fidelity closed-form formulae are developed to predict the shear modulus of hexagonal graphene-like monolayer nanostructures and nano-heterostructures based on a physically insightful analytical approach. Hexagonal nano-structural forms (top view) are common for nanomaterials with monoplanar (such as graphene, hBN) and multiplanar (such as stanene, MoS_2) configurations. However, a single-layer nanomaterial may not possess a particular property adequately, or multiple desired properties simultaneously. Recently a new trend has emerged to develop nano-heterostructures by assembling multiple monolayers of different nanostructures to achieve various tunable desired properties simultaneously. Shear modulus assumes an important role in characterizing the applicability of different two-dimensional nanomaterials and heterostructures in various nanoelectromechanical systems such as determining the resonance frequency of the vibration modes involving torsion, wrinkling and rippling behavior of two-dimensional materials. We have developed mechanics-based closed-form formulae for the shear modulus of monolayer nanostructures and multi-layer nano-heterostructures. New results of shear modulus are presented for different classes of nanostructures (graphene, hBN, stanene and MoS_2) and nano-heterostructures (graphene-hBN, graphene-MoS_2, graphene-stanene and stanene-MoS_2), which are categorized on the basis of the fundamental structural configurations. The numerical values of shear modulus are compared with the results from scientific literature (as available) and separate molecular dynamics simulations, wherein a good agreement is noticed. The proposed analytical expressions will enable the scientific community to efficiently evaluate shear modulus of wide range of nanostructures and nanoheterostructures.

Keywords: Hexagonal nanostructures; heterostructure, shear modulus; Analytical closed-form formulae; graphene-like materials

*Corresponding author: Tanmoy Mukhopadhyay (Email address: tanmoy.mukhopadhyay@eng.ox.ac.uk)

1. Introduction

A mechanics-based analytical approach is presented to derive the generalized closed-form formulae for the effective shear modulus of hexagonal multiplanar nano-structures and nano-heterostructures. With the feasible isolation of single layer carbon atoms, known as graphene [1, 2], the fascinating and unprecedented properties of this monolayer nanostructure had initiated intense research in exploration of prospective alternative two-dimensional and quasi-two-dimensional materials that could possess exciting electronic, optical, thermal, chemical and mechanical characteristics [3–9]. It is important to investigate these materials at nano-scale as most of the interesting characteristics are in atomic scale and monolayer forms [10]. Over the span of last decade the interest in such two-dimensional nanomaterials has expanded from hBN, BCN, graphene oxides to Chalcogenides (MoS_2, $MoSe_2$) and other quasi-two-dimensional materials like stanene, phosphorene, silicene, sermanene, borophene etc. [11–15]. Among different such materials, as discussed above, hexagonal nanostructural form is a prominent structural configuration [4, 16]. From a structural view-point, monolayer nanostructures can be of either monoplanar (where all the atoms are in a single plane such as graphene and hBN) or nultiplanar (where the constituent atoms lie in multiple planes such as stanene and MoS_2) configuration (refer to subsection 2.1 for detail description of monoplanar and multiplanar nanostructures).

Despite of the tremendous advancement in two-dimensional materials research, it has been realized that a single-layer nanomaterial may not possess a particular property adequately, or multiple desired properties simultaneously. Recently a new trend has emerged to develop nano-heterostructures by assembling multiple monolayers of different nanostructures to achieve various tunable desired properties simultaneously [17–20]. Although the monolayer of quasi-two-dimensional materials have hexagonal lattice nano-structure (top-view) in common, their out-of-plane lattice characteristics are quite different. Subsequently, these materials exhibit significantly different mechanical and electronic properties. For example, transition metal dichalcogenides such as MoS_2 show exciting electronic and piezoelectric properties, but their low in-plane mechanical strength is a constraint for any practical application. In contrast, graphene possesses strong in-plane mechanical properties. Moreover, graphene is extremely weak in the out-of-plane direction with a very low bending modulus, whereas the bending modulus of MoS_2 is comparatively much higher, depending on their respective single-layer thickness [21]. Having noticed that graphene and MoS_2 possess such complementary physical properties, it is a quite rational attempt to combine these two materials in the form of a graphene-MoS_2 heterostructure, which could exhibit the de-

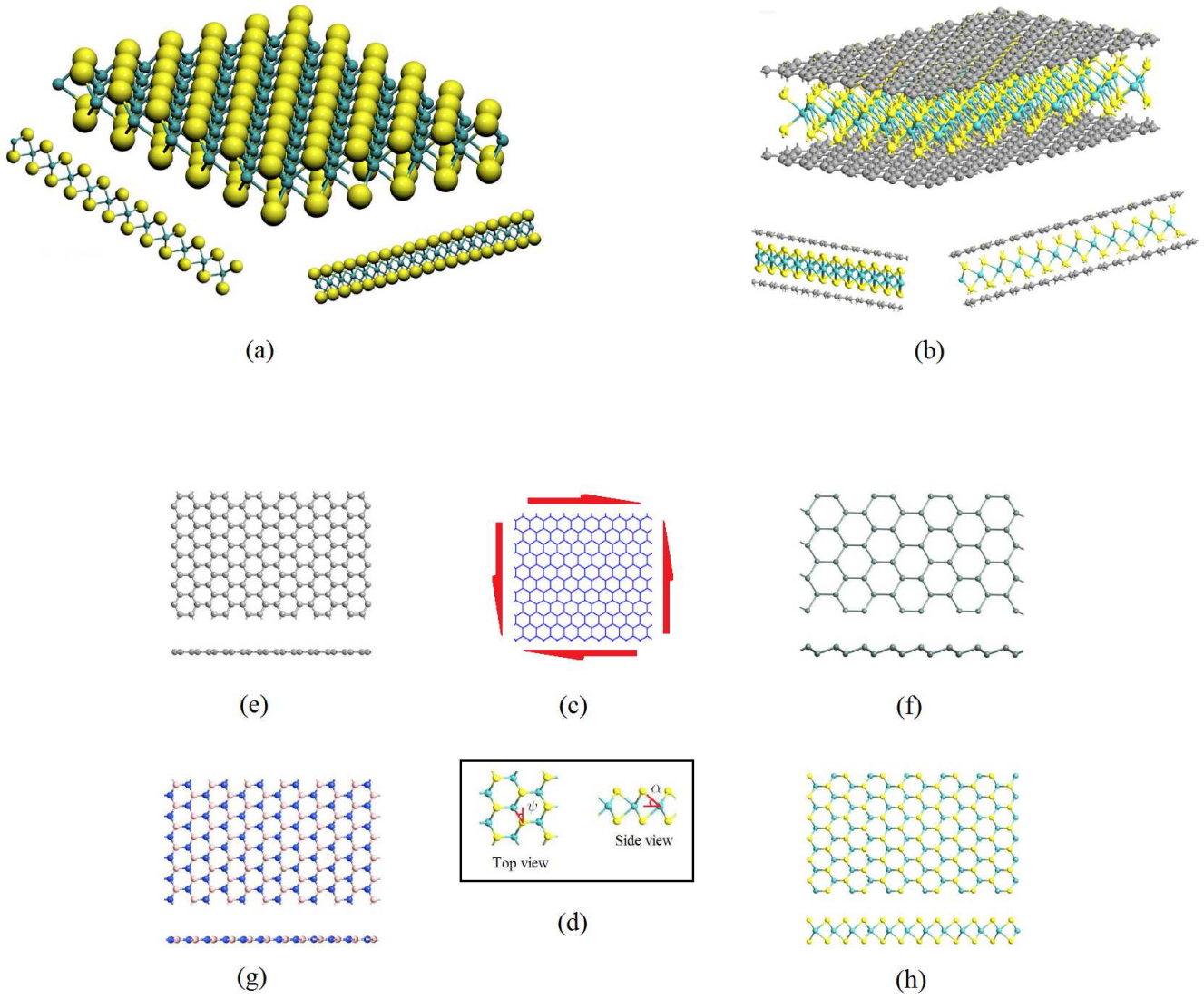

Figure 1: (a) Three dimensional view of multiplanar hexagonal nano-structures along with side views from two mutually perpendicular directions (b) Three dimensional view of nano-heterostructure structure (having three layers consisting of a multiplanar layer sandwiched between two monoplanar layers at top and bottom) along with side views from two mutually perpendicular directions (c) A typical representation of hexagonal two-dimensional nanostructures subjected to in-plane shear stress (d) Top and side view of a generalized hexagonal nanostructural form (e) Top and side view of single-layer hexagonal nanostructures where all the constituent atoms are same and they are in a single plane (Class I: e.g. graphene) (f) Top and side view of single-layer hexagonal nanostructures where the constituent atoms are same but they are in two different planes (Class II: e.g. silicene, germanene, phosphorene, stanene, borophene) (g) Top and side view of single-layer hexagonal nanostructures where the constituent atoms are not same but they are in a single plane (Class III: e.g. hBN, BCN) (h) Top and side view of single-layer hexagonal nanostructures where the constituent atoms are not same and they are in two different planes (Class IV: e.g. MoS_2, WS_2, $MoSe_2$, WSe_2, $MoTe_2$)

sired level of electronic properties and in-plane as well as out-of-plane strengths. Besides intense research on different two-dimensional hexagonal nano-structural forms, recently the development of novel application-specific heterostructures has started receiving considerable attention from the scientific community due to the tremendous prospect of combining different single layer materials

in intelligent and intuitive ways to achieve several such desired physical and chemical properties [22–30].

For understanding the structural performance of the nanostructures and nano-heterostructures (intended to be utilized as nanoelectromechanical systems such as resonators or nanosensors) from a mechanical strength view-point, it is of utmost importance to evaluate their Young's moduli, Poisson's ratios and shear modulus. While closed-form analytical expressions are reported in literature for Young's moduli and Poisson's ratios of multiplanar structural forms and nanoheterostructures [31, 32], there is no such efficient formulae available yet for the shear modulus of nanostructure and nano-heterostructures. Shear modulus assumes a vital role in evaluating the resonance frequency of the vibration modes involving torsion. Such torsional modes have been reported to have advantage over the flexural modes for the absence of thermoelastic loss leading to an improvement in mechanical quality factors and device sensitivity. The shear deformation is also important in characterizing the wrinkling and rippling behaviour of two-dimensional materials that controls the charge carrier scattering property and electron mobility [33].

The common computational approaches to investigate two-dimensional nanomaterials are first principle studies/ ab-initio [34–39], molecular dynamics [40] and molecular mechanics [41], which are capable of reproducing the results of experimental analysis. First principle studies/ ab-initio and molecular dynamics based material characterization approaches are normally expensive and time consuming. Moreover, availability of interatomic potentials can be a practical barrier in carrying out molecular dynamics simulation for nano-heterostructures, which are consisted of multiple materials. The mechanics-based analytical approach of evaluating elastic moduli is computationally very efficient, yet it produces accurate. Analytical models leading to efficient closed-form formulae are presented by many researchers for materials with monoplanar hexagonal nano-structures [42–45], while shear modulus of multiplanar structures are not found to be adequately addressed. The research in the field of nano-heterostructures is still in a very nascent stage and investigations on elastic properties of such built-up structural forms is very scarce to find in literature [22, 23, 46], wherein the predominant approach for evaluating the elastic moduli is expensive molecular dynamics simulation. To reach the full potential of such nano-scale built-up structural form, it is essential to develop computationally efficient closed-form formulae for the effective elastic properties of nano-hetrostructures that can serve as a ready reference for the researchers without the need of conducting expensive and time consuming molecular dynamics simulation or laboratory experiments. Since shear modulus of different two-dimensional nanomaterials and heterostructures

are very scarce to find in literature, there exists a strong rationale to develop a generalized analytical model leading to efficient and closed-form, yet high fidelity expressions for obtaining the shear modulus of such natural and artificial nanomaterials.

Aim of the present paper is to cater on the need for developing an efficient physics-based framework that can obtain the shear modulus of wide range of monolayer nanostructures (monoplanar and multiplanar) and nano-heterostructures (with any stacking configuration). This article hereafter is organized as follows: analytical formulae for the shear modulus of nano-scale materials with multiplanar hexagonal nano-structures and nano-heterostructures are derived in section 2; results and relevant discussions on the developed analytical approach is provided in section 3 along with validation of the developed formulae for four different single-layer materials belonging to four different classes (graphene, hBN, stanene and MoS_2) and four different heterostructures belonging to the three categories (graphene-hBN, stanene-MoS_2, graphene-stanene and graphene-MoS_2); a summary of the important observations made from results and perspective of this work in the context of contemporary researches is discussed in section 4 and finally conclusion and scope of future researches based on this work is presented in section 5.

2. Shear modulus of hexagonal nanostructures and heterostructures

Generalized closed-form mechanics-based formulae for the shear modulus of hexagonal nanostructures (applicable to both monoplanar and multiplanar structural forms) and nano-heterostructures (applicable to any number of layers and stacking sequence) are developed in this section. After a concise discussion of the structural classification of nanomaterials, the equivalent elastic properties of the atomic bonds are described; thereby the closed-form expressions of the shear modulus are derived. The approach for obtaining the equivalent elastic properties of atomic bonds is well-established in scientific literature [32, 41, 43, 47, 48]. Therefore, the main contributing of this work lies in development of the analytical formulae for shear modulus of monoplanar and multiplanar hexagonal nanostructures and nano-heterostructures. In this context, it can be noted that the mechanics of honeycomb-like structural form is investigated extensively in micro and macro scales based on principles of structural mechanics [49–55].

2.1. Classification of hexagonal nanomaterials based on structural configuration

On the basis of structural configuration, monolayer two-dimensional materials can be classified in four different classes as shown in figure 1(d–g) [32]. For example, graphene [42] consists of a single type of atom (carbon) to form a hexagonal honeycomb-like lattice structure in one single plane,

while there is a different class of materials that possess hexagonal monoplanar nanostructure with different constituent atoms such as hBN [44], BCN [56] etc. Unlike these monoplanar hexagonal nanostructures, there are plenty of other materials having the constituent atoms placed in multiple planes to form a hexagonal top view. Such multiplanar hexagonal nanostructures may be consisted of either a single type of atom (such as stanene [57], silicene [58], germanene [58], phosphorene [59], borophene [60] etc.), or different atoms (such as MoS_2 [61–63], WS_2 [64], $MoSe_2$ [65], WSe_2 [64], $MoTe_2$ [66] etc.). However, from a mechanics point-of-view, two separate categories are required to be recognised: monoplanar structures (where all the constituent atoms are in a single plane, such as graphene and hBN) and multiplanar structures (where all the constituent atoms are in different planes, such as stanene and MoS_2). This is because of the fact that the equivalent properties of the bonds are important in evaluating the elastic properties of materials, rather than the similarity or dissimilarity of two adjacent atoms. It can be noted in this context that the monoplanar structural form can be treated as a special case of multiplanar structures. The top view and side view of a general multiplanar hexagonal nanostructure are shown in figure 1(d). From the figure, it is evident that a multiplanar structure reduces to monoplanar form when the out-of-plane angle becomes zero (i.e. $\alpha = 0$).

From a structural perspective, the hexagonal nano-heterostructures can be broadly classified into three categories: heterostructure containing only mono-planar nanostructures (such as graphene-hBN heterostructure [24, 25, 67]), heterostructure containing both mono-planar and multi-planar nanostructures (such as graphene-MoS_2 heterostructure [21, 23], graphene-stanene heterostructure [26], phosphorene-graphene heterostructure [68], phosphorene-hBN heterostructure [68], multi-layer graphene-hBN-TMDC heterostructure [28]) and heterostructure containing only multi-planar nanostructures (such as stanene-MoS_2 heterostructure [27], MoS_2-WS_2 heterostructure [22]).

2.2. Mechanical equivalence of atomic bonds

For atomic level behaviour of nano-scale materials, the effective interatomic potential energy can be evaluated as a sum of various individual energy components related to bonding and non-bonding interactions [41]. Total strain energy (E) consists of the contributions from bending of bonds (E_b), bond stretching (E_s), torsion of bonds (E_t) and energies associated with non-bonded terms (E_{nb}) such as the van der Waals attraction, the core repulsions and the coulombic energy

$$E = E_s + E_b + E_t + E_{nb} \tag{1}$$

However, among all the energy components, effect of bending and stretching are predominant in case of small deformation [43, 47]. For the multiplanar hexagonal nano-structures (such as

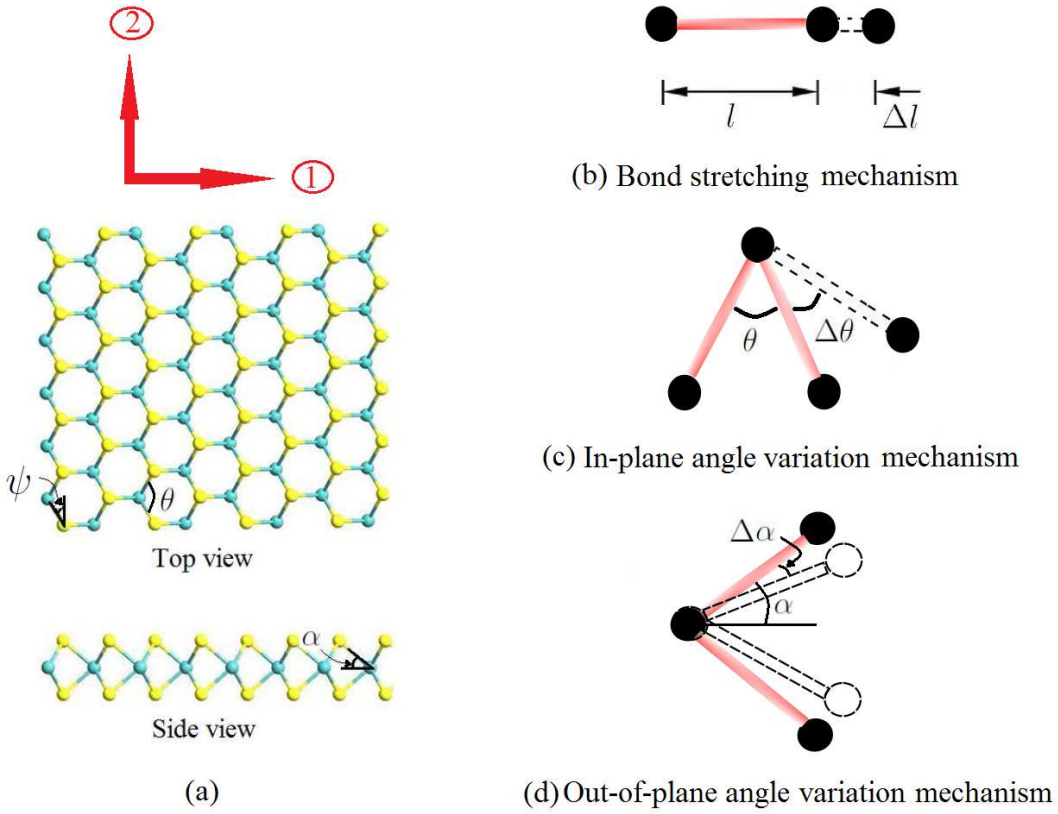

Figure 2: (a) Top and side view of a multiplanar hexagonal nanostructure (b) Deformation mechanism of bond stretching (c) Deformation mechanism of in-plane (1-2 plane) angle variation (d) Deformation mechanism of out-of-plane (normal to the 1-2 plane) angle variation

stanene and MoS_2), the strain energy pertaining to bending consists of two components: in-plane component (E_{bI}) and out-of-plane component (E_{bO}). The predominant deformation mechanisms for a multiplanar nanostructure are depicted in figure 2. It can be noted that the out-of-plane component becomes zero for monoplanar nanostructures such as graphane and hBN. The total inter-atomic potential energy (E) can be expressed as

$$\begin{aligned} E &= E_s + E_{bI} + E_{bO} \\ &= \frac{1}{2}k_r(\Delta l)^2 + \left(\frac{1}{2}k_\theta(\Delta\theta)^2 + \frac{1}{2}k_\theta(\Delta\alpha)^2\right) \end{aligned} \tag{2}$$

where Δl, $\Delta\theta$ and $\Delta\alpha$ denote the change in bond length, in-plane angle and out-of-plane angle respectively, as shown in figure 2. The quantities k_r and k_θ represent the force constants related to bond stretching and bending respectively. The first term in Equation 2 corresponds to strain energy due to stretching (E_s), while the terms within bracket represent the strain energies due to in-plane angle (E_{bI}) and out-of-plane (E_{bO}) angle variations, respectively. The force constants of the atomic bonds (k_r and k_θ) can be expressed in the form of structural equivalence [69]. As per the standard theory of structural mechanics, the strain energy of a uniform circular beam having length

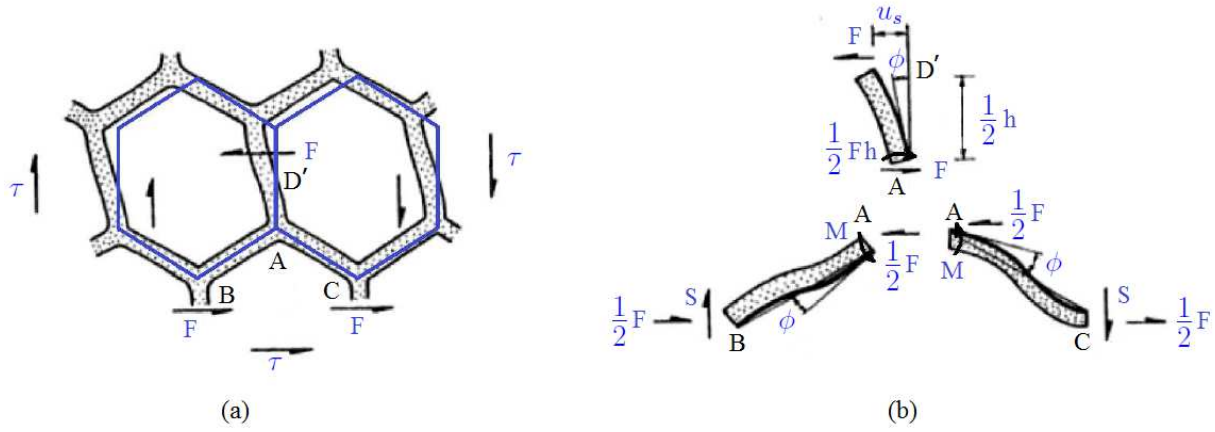

Figure 3: Top view of a multi-planar hexagonal lattice for deriving the in-plane shear modulus

l, cross-sectional area A, second moment of area I and Young's modulus E, under the application of a pure axial force N, can be expressed as

$$U_a = \frac{1}{2}\int_0^L \frac{N^2}{EA}\,\mathrm{d}l = \frac{1}{2}\frac{N^2 l}{EA} = \frac{1}{2}\frac{EA}{l}(\Delta l)^2 \tag{3}$$

The strain energies due to pure bending moment M causing a slope of $\Delta\phi$ at the end points of the beam [32] can be written as

$$U_b = \frac{1}{2}\int_0^L \frac{M^2}{EI}\,\mathrm{d}l = \frac{1}{2}\frac{EI}{l}(2\Delta\phi)^2 \tag{4}$$

Comparing Equation 3 with the expression for strain energy due to stretching (E_s) (refer to Equation 2), it can be concluded that $K_r = \dfrac{EA}{l}$. For bending, it is reasonable to assume that $2\Delta\phi$ is equivalent to $\Delta\theta$ and $\Delta\alpha$ for in-plane and out-of-plane angle variations respectively. Thus comparing Equation 4 with the expressions for the strain energies due to in-plane (E_{bI}) and out-of-plane (E_{bO}) angle variations, the following relation can be obtained: $k_\theta = \dfrac{EI}{l}$. On the basis of the established mechanical equivalence between molecular mechanics parameters (k_r and k_θ) and structural mechanics parameters (EA and EI), the effective shear modulus of monolayer nanostructures and nano-heterostructures are obtained in the following subsections.

2.3. Shear modulus of mono-layer quasi-two-dimensional hexagonal nanostructures

For deriving the in-plane shear modulus of multiplanar hexagonal nanostructures, the free body diagram shown in figure 3 is analysed. It should be noted here that the top view is shown in this figure and the individual constituent members are inclined at an angle α as described in figure 1(c). Analysing the free body diagram presented in figure 3(b)

$$M = \frac{Fl\cos\alpha}{4} \tag{5}$$

where $F = 2\tau l^2 \cos\psi \cos\alpha \sin\alpha$. Deflection of the end A with respect to the end C under the application of moment M at the point A is given as

$$\delta_0 = \frac{Ml^2}{6EI} \tag{6}$$

Thus the rotation of joint A can be expressed as

$$\begin{aligned} \phi &= \frac{\delta_0}{l} \\ &= \frac{Fl^2 \cos\alpha}{24EI} \end{aligned} \tag{7}$$

Deformation of point D' in the direction of F due to rotation of the joint A is

$$\delta_r = \frac{1}{2}\phi l = \frac{Fl^3 \cos\alpha}{48EI} \tag{8}$$

The bending deformation of the member AD' in the direction of F can be expressed as

$$\delta_b = \frac{Fl^3}{24EI} \tag{9}$$

The total shear deformation due to bending of the member AD' and rotation of the joint A is given by

$$u_s = \delta_b + \delta_r = \frac{Fl^3}{48EI}(\cos\alpha + 2) \tag{10}$$

The axial deformation of members AB and AC caused by the force S will also contribute to the total shear deformation, where $S = \tau l^2 \sin\alpha \cos\alpha(1 + \sin\psi)$. Comparing the expression of τ, obtained from the expressions of F and S

$$S = \frac{F(1 + \sin\psi)}{2\cos\psi} \tag{11}$$

Axial deformation of the member AB can be expressed as (Refer to figure 2(a) for the in-plane and out-of-plane angles ψ and α respectively. Figure 3(b) shows the application of two forces S and $\frac{F}{2}$ on the member AB)

$$\begin{aligned} \delta_a &= \frac{\left(S\sin\psi + \frac{F}{2}\cos\psi\right)\cos\alpha l \cos\alpha \sin\psi}{AE} \\ &= \frac{Fl\sin\psi(1 + \sin\psi)\cos^2\alpha}{2AE\cos\psi} \end{aligned} \tag{12}$$

Based on the force components shown in the free body diagrams of figure 3(b), the axial deformation of members AB and AC would have same numerical value, but opposite nature. Thus the total shear strain component caused by the axial deformation of the members AB and AC can be expressed as

$$\gamma_a = \frac{2\delta_a}{2l\cos\psi\cos\alpha} \tag{13}$$

The shear strain component caused by the bending deformation of the member AD' and rotation of the joint A is given by

$$\gamma_b = \frac{u_s}{l(1+\sin\psi)\cos\alpha} \tag{14}$$

Substituting the expressions of δ_a and u_s from Equation 12 and 10 respectively, the total shear strain caused by bending and axial deformations for an entire hexagonal unit (as shown in figure 3(a)) can be obtained as [49]

$$\begin{aligned}\gamma &= 2(\gamma_a + \gamma_b) \\ &= \tau l^2 \cos\psi \cos\alpha \sin\alpha \left(\frac{\sin\psi(1+\sin\psi)}{AE\cos^2\psi} + \frac{l^2(\cos\alpha+2)}{6EI(1+\sin\psi)\cos\alpha} \right)\end{aligned} \tag{15}$$

Replacing the structural mechanics parameters EI and AE by the molecular mechanics parameters k_θ and k_r respectively ($K_r = \frac{EA}{l}$ and $k_\theta = \frac{EI}{l}$) in the above equation, the expression for in-plane shear modulus can be expressed as

$$\begin{aligned}G_{12} &= \frac{\tau}{\gamma} \\ &= \frac{k_r k_\theta \cos\psi(1+\sin\psi)}{t\left(k_\theta \sin\psi(1+\sin\psi)^2\cos\alpha + \frac{k_r l^2}{6}\cos^2\psi(\cos\alpha+2) \right)}\end{aligned} \tag{16}$$

In the above expression $\psi = 90^\circ - \frac{\theta}{2}$, where θ is the bond angle as shown in figure 2(a).

2.4. Effective shear modulus of multi-layer hexagonal nano-heterostructures

Equivalent shear modulus of the nano-heterostructures are derived based on a multi-stage bottom-up idealization scheme as depicted in figure 4. In the first stage, the effective shear modulus of each individual layer is determined based on a mechanics-based approach using the mechanical equivalence of bond properties as described in the preceding subsection. Thus the multi-layer heterostructure can be idealized as a layered plate-like structural element with respective effective shear modulus and geometric dimensions (such as thickness) of each layer. Each of the layers are considered to be bonded perfectly with adjacent layers. The equivalent shear modulus of the whole nano-heterostructure is determined based on force equilibrium and deformation compatibility based conditions at the final stage.

Figure 5 shows the typical representation of an idealized three-layer heterostructure with the in-plane shear stress applied in 1-2 plane. From the condition of force equilibrium, the total shear force should be equal to the summation of the shear force component shared by each of the constituting layers. Thus considering a heterostructure with n number of layers

$$\tau t L = \sum_{i=1}^{n} \tau i t_i L \tag{17}$$

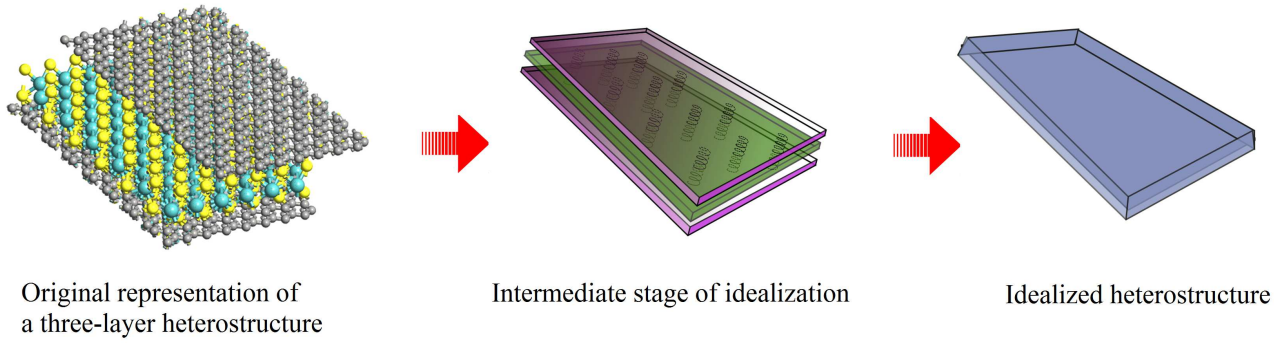

Figure 4: Idealization scheme for the analysis of a typical three-layer nano-heterostructure

From the definition of shear modulus, the above expression can be written as

$$G_{12}\gamma t = \sum_{i=1}^{n} G_{12i}\gamma_i t_i \tag{18}$$

where G_{12} and γ are the effective shear modulus and the shear strain respectively for the entire heterostructure. G_{12i} and γ_i represent the effective shear modulus and the shear strain of i^{th} layer respectively. As each of the layers are considered to be perfectly bonded with the adjacent layers, the deformation compatibility condition yields: $\gamma = \gamma_i, \in [1, n]$. Thus Equation 18 and 16 give the expression of in-plane shear modulus for the entire heterostructure as

$$\begin{aligned} G_{12} &= \frac{1}{t}\sum_{i=1}^{n} G_{12i}t_i \\ &= \frac{1}{t}\sum_{i=1}^{n} \frac{k_{ri}k_{\theta i}\cos\psi_i(1+\sin\psi_i)}{\left(k_{\theta i}\sin\psi_i(1+\sin\psi_i)^2\cos\alpha_i + \frac{k_{ri}l_i^2}{6}\cos^2\psi_i(\cos\alpha_i+2)\right)} \end{aligned} \tag{19}$$

The subscript i in the above expression of G_{12} indicates the molecular mechanics and structural (/geometrical) properties corresponding to the i^{th} layer. Here t denotes the total thickness of the heterostructure.

2.5. Remark 1: Non-dimensionalization of shear modulus for monolayer nanostructures

The physics based analytical formulae developed in this article are capable of providing an comprehensive understanding of the behaviour of multiplanar hexagonal nano-structures. Non-dimesional quantities in physical systems can cater to an insight for wide range of nano-scale materials. The expression for shear modulus, as presented in Equation 16, can be rewritten in terms of non-dimensional parameters as

$$\tilde{G}_{12} = \frac{\cos\psi(1+\sin\psi)}{(\sin\psi(1+\sin\psi)^2\cos\alpha + 2\lambda\cos^2\psi(\cos\alpha+2))} \tag{20}$$

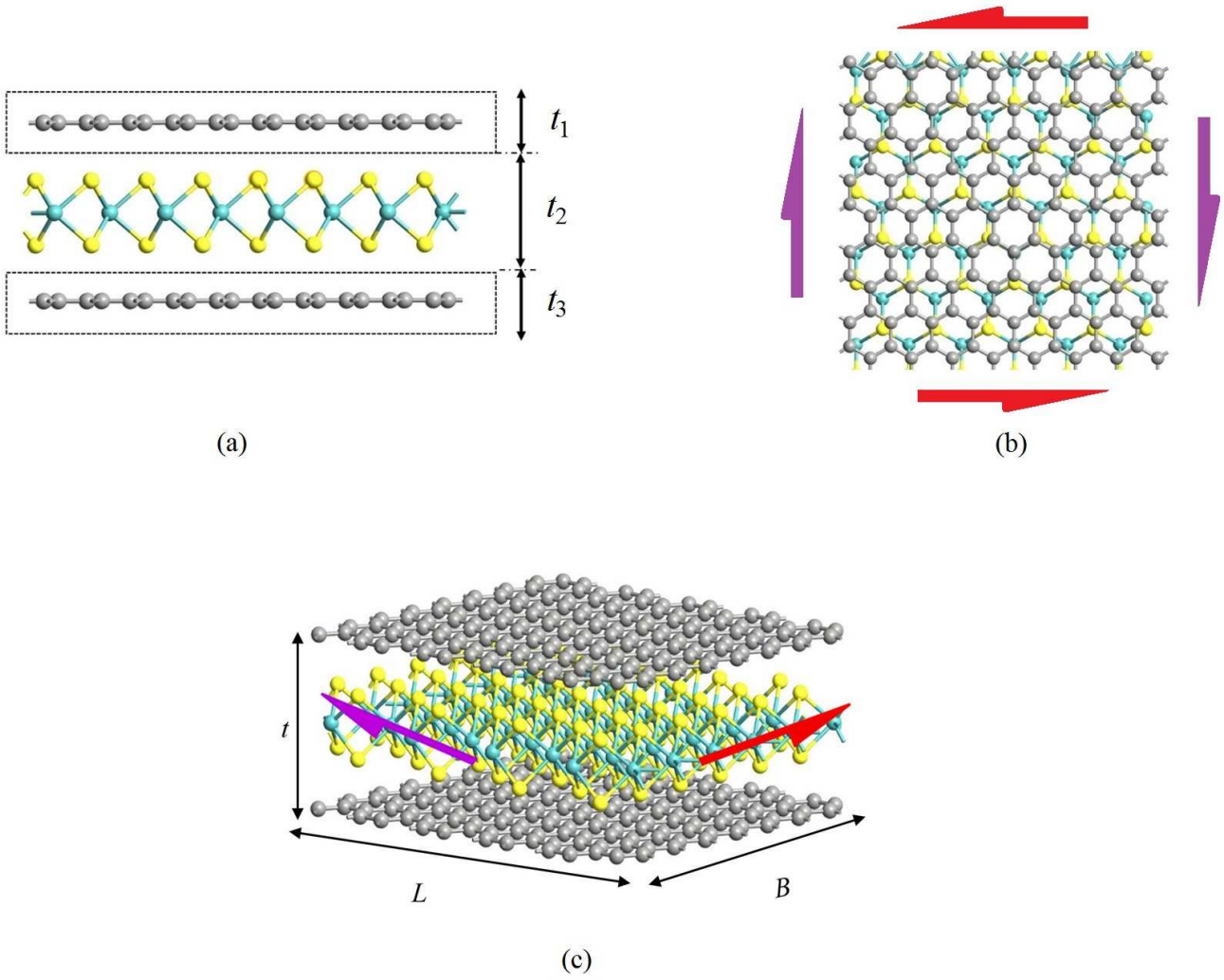

Figure 5: (a) Side view of a typical three-layer heterostructure (b) Application of shear stress in nano-heterostructures (top view) (c) Application of shear stress in nano-heterostructures (three-dimensional view)

where λ $(= \frac{l^2}{12}\frac{k_r}{k_\theta})$ is a non-dimensional aspect ratio measure of the bonds that is found to vary in the range of 0.4 to 2.8 for common materials with hexagonal nanostructures. It is interesting to notice that λ reduces to $\frac{4}{3}\left(\frac{l}{d}\right)^2$ using the definition of k_r and k_θ, where l and d are the bond length and bond diameter respectively. Thus the parameter λ is a measure of the aspect ratio of the bonds in hexagonal nano-structure. Here $\tilde{G_{12}} = \frac{G_{12}t}{k_r}$ is the non-dimensional representation of the shear modulus. Thus the non-dimensional shear modulus depend on the aspect ratio of the bond, in-plane and out-of-plane angles. Results are presented in section 3 considering the non-dimensional quantities for in-depth mechanical characterization of hexagonal nanostructures.

2.6. Remark 2: Special case for monoplanar nanostructures

For the hexagonal nanostructures with monoplanar configuration (e.g. graphene and hBN), α becomes 0. The shear modulus for such materials can be expressed as (substituting $\alpha = 0$ in

Equation 16)

$$G_{12} = \frac{k_r k_\theta \cos\psi(1+\sin\psi)}{t\left(k_\theta \sin\psi(1+\sin\psi)^2 + \frac{k_r l^2}{2}\cos^2\psi\right)} \tag{21}$$

However, for regular hexagonal nano-structures (such as graphene), the bond angle (θ) is 120°. Thus replacing $\psi = 30°$, the Equation 21 yields a simple expression as

$$G_{12} = \frac{2\sqrt{3}k_\theta k_r}{t(3k_\theta + k_r l^2)} \tag{22}$$

2.7. Remark 3: Effective shear modulus of nano-heterostructures

The expression for the shear modulus of nano-heterostructures derived in the preceding section (Equation 19) reduce to the expression provided for a single layer of nanostructure (Equation 16) in case of $n = 1$. The derived closed-form expressions for nano-heterostructures are capable of obtaining the shear modulus corresponding to any stacking sequence of the constituent layer of nano-materials, including the heterostructures consisted of multiple materials [28]. Such generalization in the derived formulae, with the advantage of being computationally efficient and easy to implement, opens up a tremendous potential scope in the field of novel application-specific heterostructure development.

An advantage of the proposed bottom-up approach of considering layer-wise equivalent material property is that it allows us to neglect the effect of lattice mismatch in evaluating the effective shear modulus for multi-layer heterostructures consisting of different materials. In the derivation for effective shear modulus of such heterostructues, the deformation compatibility conditions of the adjacent layers are satisfied. This is expected to give rise to some strain energy locally at the interfaces, which is noted in previous studies [23]. From the derived expressions it can be discerned that the numerical values of the shear modulus actually depends on the number of layers of different constituent materials rather than their stacking sequences. In case of multi-layer nanostructures constituted of the layers of same material (i.e. bulk material), it can be expected from Equation 19 that the shear modulus would reduce owing to the presence of inter-layer distances, which, in turn, increase the value of overall thickness t.

3. Results and discussion

3.1. Equivalent bond parameters and structural configurations of nanostructures

Four different materials with hexagonal nano-structures (graphene, hBN, stanene and MoS_2) and heterostructures formed by these four materials are considered in this paper to present results based

on Equation 16 and Equation 19. The molecular mechanics parameters and geometric properties of the bonds (k_r, k_θ, bond length in-plane and out-of-plane bond angles for different materials), which are required to obtain the shear modulus using the proposed approach, are well-documented in scientific literature. In case of graphene, the molecular mechanics parameters k_r and k_θ can be obtained from literature using AMBER force filed [70] as $k_r = 938$ kcal mol^{-1}nm$^{-2} = 6.52 \times 10^{-7}$ Nnm^{-1} and $k_\theta = 126$ kcal mol^{-1}rad$^{-2} = 8.76 \times 10^{-10}$ Nnm rad^{-2}. The out-of-plane angle for graphene is $\alpha = 0$ and the bond angle is $\theta = 120^\circ$ (i.e. $\psi = 30^\circ$), while bond length and thickness of single-layer graphene can be obtained from literature as 0.142 nm and 0.34 nm respectively [42]. In case of hBN, the molecular mechanics parameters k_r and k_θ can be obtained from literature using DREIDING force model [71] as $k_r = 4.865 \times 10^{-7}$ Nnm^{-1} and $k_\theta = 6.952 \times 10^{-10}$ Nnm rad^{-2} [72]. The out-of-plane angle for hBN is $\alpha = 0$ and the bond angle is $\theta = 120^\circ$ (i.e. $\psi = 30^\circ$), while bond length and thickness of single-layer hBN can be obtained from literature as 0.145 nm and 0.098 nm respectively [44]. In case of stanene, the molecular mechanics parameters k_r and k_θ can be obtained from literature as $k_r = 0.85 \times 10^{-7}$ Nnm^{-1} and $k_\theta = 1.121 \times 10^{-9}$ Nnm rad^{-2} [73, 74]. The out-of-plane angle for stanene is $\alpha = 17.5^\circ$ and the bond angle is $\theta = 109^\circ$ (i.e. $\psi = 35.5^\circ$), while bond length and thickness of single layer stanene can be obtained from literature as 0.283 nm and 0.172 nm respectively [73–76]. In case of MoS_2, the molecular mechanics parameters k_r and k_θ can be obtained from literature as $k_r = 1.646 \times 10^{-7}$ Nnm^{-1} and $k_\theta = 1.677 \times 10^{-9}$ Nnm rad^{-2}, while the out-of-plane angle, bond angle, bond length and thickness of single layer MoS_2 are $\alpha = 48.15^\circ$, $\theta = 82.92^\circ$ (i.e. $\psi = 48.54^\circ$), 0.242 nm and 0.6033 nm respectively [61, 77–79].

3.2. Shear modulus of single-layer hexagonal nano-structures

The proposed expression for shear modulus is generalized in nature and they can be applicable for a wide range of materials having hexagonal nano-structural forms by providing respective structural parameters as input. Four different materials with hexagonal nano-structures are considered (graphene, hBN, stanene and MoS_2) that have monoplanar as well as multiplanar structural forms. Comparative results for the shear modulus is presented in Table 1 as $\bar{G_{12}} = G_{12} \times t$ with unit TPa-nm (tensile rigidity), where t is the single layer thickness [41, 44]. Thus the exact numerical values of shear modulus (G_{12} in TPa) can be evaluated by dividing the presented values ($\bar{G_{12}}$) with unit TPa-nm) by the respective single-layer thickness (t in nm). It is found from scientific literature that shear modulus of monoplanar nanomaterials such as graphene and hBN have been investigated in previous studies (refer to Table 1), while no result for shear modulus is found for multiplanar structural forms (such as stanene and MoS_2). Thus, to validate the proposed analytical formula for

Table 1: Results for the shear modulus of single-layer materials (Results are presented as $\bar{G_{12)}} = G_{12} \times t$ (unit TPa-nm), where t is the single layer thickness of a particular nanomaterial. Reference results are obtained from literature for graphene and hBN, while seperate molecular dynamics (MD) simulation is carried out for MoS_2.)

Material	Present Results	Reference results
Graphene (Monoplanar)	$\bar{G_{12}} = 0.1254$	0.0724–0.0741 [80], 0.1676 [81] 0.0952±0.0122 [33]
hBN (Monoplanar)	$\bar{G_{12}} = 0.0951$	0.0951 [82], 0.105 [83] , 0.165 [84]
Stanene (Multiplanar)	$\bar{G_{12}} = 0.0325$	–
MoS_2 (Multiplanar)	$\bar{G_{12}} = 0.0719$	0.079 [MD]

single-layer of monoplanar nanostructures, we have compared the results with available numerical values of shear modulus in literature. However, to validate the analytical formulae for multiplanar single-layer nanostructures, separate molecular dynamics simulation is carried out for MoS_2, which has a multiplanar nanostructure. Having the proposed closed-form formulae validated for both monoplanar as well as multiplanar nanostructures, the shear modulus is predicted for single-layer stanene having a multiplanar nanostructural form. The results of shear modulus are presented in Table 1 for graphene, hBN, stanene and MoS_2, wherein a good agreement is noticed between the analytical predictions and reference results obtained from scientific literature and molecular dynamics simulation.

The molecular dynamics simulations for the shear modulus are performed on $10 \times 10 \times 10$ super cell for all the two-dimensional nanostructures and nano-heterostructures in LAMMPS [85]. AIREBO (adaptive intermolecular reactive empirical bond order) potential is used for graphene [86] and REBO (reactive empirical bond-order) potential is used for MoS_2 [87]. Both REBO and AIREBO potentials have been shown to accurately capture the bond-bond interaction between carbon atoms and molybdenum-sulfur atoms for single-layer two-dimensional structures. In order to terminate the bond-order potential to the nearest neighbour interactions, a cut-off function is

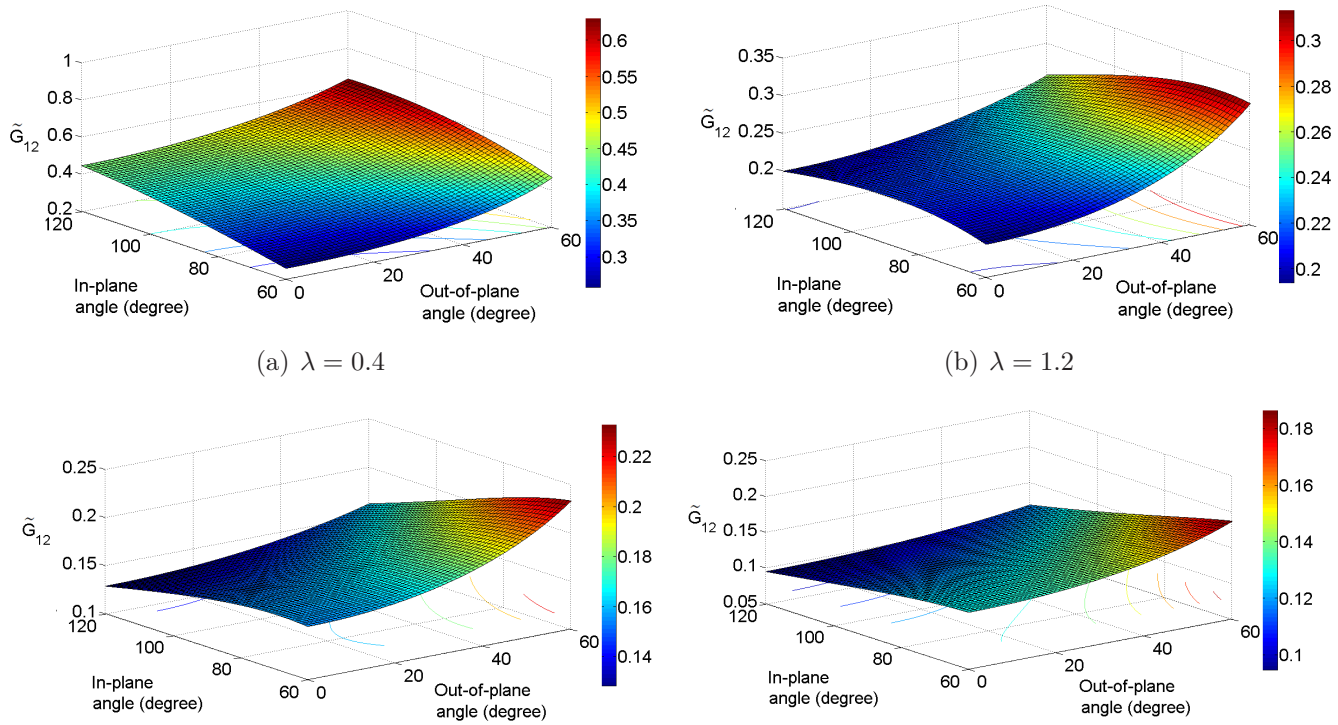

(a) $\lambda = 0.4$ (b) $\lambda = 1.2$

(c) $\lambda = 2.0$ (d) $\lambda = 2.8$

Figure 6: Variation of shear modulus with in-plane angle (θ) and out-of-plane angle (α). Here $\lambda = \dfrac{l^2 k_r}{12 k_\theta}$, $\tilde{G_{12}} = \dfrac{G_{12} t}{k_r}$, where l and t are the bond length and single-layer thickness, respectively.

found to be used in most empirical potentials. We have set the cut-off parameter as $2.0\dot{A}$ for the REBO part of the potential, as suggested in various previous publications [88, 89]. AIREBO for graphene [90, 91] and REBO for MoS_2 [92, 93] are found to be widely used for mechanical properties and failure analyses. It is expected to predict the shear modulus accurately; our analytical prediction gives close result with respect to the numerical values obtained from molecular dynamics simulation (refer to Table 1).

The physics-based analytical formulae presented in this paper for the shear modulus of monolayer nanostructures are capable of providing a thorough insight encompassing wide range of materials. Variations of the shear modulus (G_{12}) with in-plane and out-of-plane angles (θ and α) for different values of the aspect ratio measure (λ) is presented in figure 6 using the non-dimensional parameters as described in subsection 2.5. The aspect ratio measure of the bonds (λ) varies in the range of 0.4 to 2.8 for common materials with hexagonal nano-structures (specifically in case of the four considered materials: $\lambda = 1.2507, 2.495, 0.5061, 0.479$ for graphene, hBN, stanene and MoS_2 respectively). The results for the shear modulus is presented for $\lambda = 0.4, 1.2, 2.0, 2.8$. Such plots can readily provide the idea about the shear modulus of any material with hexagonal nano-structure in a comprehensive

Table 2: Results for shear modulus (G_{12}, in Tpa) of graphene-MoS_2 (G – M) heterostructure with different stacking sequences (The thickness of single-layer of graphene and MoS_2 are considered as 0.34 nm and 0.6033 nm, respectively. Reference results are obtained from literature (if available) and separate molecular dynamics (MD) simulation)

Configuration	Present results	Reference results
G	0.3689	0.28±0.036 [33], 0.493 [81]
G/G	0.3689	0.3730 [MD]
M	0.1192	0.1310 [MD]
M/M	0.1192	0.1205 [MD]
G/M	0.2092	0.2400 [MD]
G/M/G	0.2515	0.2430 [MD]
M/G/M	0.1741	0.1685 [MD]

manner; exact values of which can be easily obtained using the proposed computationally efficient closed-form formulae.

3.3. Elastic moduli for multi-layer hexagonal nano-heterostructures

In this section, results are provided for the shear modulus of hexagonal multi-layer nano-heterostructures. As investigations on nano-heterostructures is a new and emerging field of research, the results available for the elastic moduli of different forms of heterostructures is very scarce in scientific literature. We have considered four different nano-heterostructures to present the results: graphene-MoS_2 [22, 23], graphene-hBN [24, 25, 94], graphene-stanene [26] and stanene-MoS_2 [27] (belonging to the three categories as depicted in the introduction section). Though all these four heterostructures have received attention from the concerned scientific community for different physical and chemical properties recently, only the graphene-MoS_2 heterostructure has been investigated for the Young's modulus among all other elastic moduli [24, 25]. As shear modulus of heterostructures have not been investigated yet, we have presented new results for graphene-MoS_2, graphene-hBN, graphene-stanene and stanene-MoS_2 heterostructures based on the analytical formula presented in Equation 19.

The proposed closed-form formula (Equation 19) for shear modulus of nano-heterostructures is validated for different stacking sequence of graphene-MoS_2 heterostructures by carrying out

Table 3: Results for shear modulus (G_{12}, in Tpa) of graphene-hBN (G – H), graphene-stanene (G – S) and stanene-MoS_2 (S – M) heterostructures with different stacking sequences (The single-layer thickness of graphene, hBN, stanene and MoS_2 are considered as 0.34 nm, 0.33 nm, 0.172 nm and 0.6033 nm, respectively)

G–H heterostructure		G–S heterostructure		S–M heterostructure	
Configuration	G_{12}	Configuration	G_{12}	Configuration	G_{12}
G	0.3689	G	0.3689	S	0.1890
G/G	0.3689	G/G	0.3689	S/S	0.1890
H	0.2883	S	0.1890	M	0.1192
H/H	0.2883	S/S	0.1890	M/M	0.1192
G/H	0.3292	G/S	0.3085	S/M	0.1347
G/H/G	0.3426	G/S/G	0.3326	S/M/S	0.1446
H/G/H	0.3157	S/G/S	0.2784	M/S/M	0.1279

separate molecular dynamics simulation (refer to Table 2). For molecular dynamics simulation of the nano-heterostructures Lennard-Jones (LJ) parameters are used for van der Waals interactions between carbon-carbon [95] and Carbon-Molybdenum-sulfur [96]. The LJ parameters for nano-heterostructures are verified for mechanical properties such as young modulus, bending modulus, ultimate strain and fracture strength [97]. Thus, having the derived formula for shear modulus of nano-heterostructures validated, new analytical results are presented for graphene-hBN, graphene-stanene and stanene-MoS_2 heterostructures considering different stacking sequences (refer to Table 3). The results of shear modulus corresponding to various stacking sequences are noticed to have an intermediate value between the respective shear modulus for single-layer of the constituent materials, as expected on a logical basis. The derived closed-form expressions for nano-heterostructures are capable of obtaining the shear modulus corresponding to any stacking sequence of the constituent layer of nanomaterials. However, from the expressions it can be discerned that the numerical value of shear modulus actually depends on the number of layers of different constituent materials rather than their stacking sequences. From a mechanics view-point, this is because of the fact that the in-plane properties are not a function of the distance of individual constituent layers from the neutral plane of the entire heterostructure. The externally applied in-plane shear force is

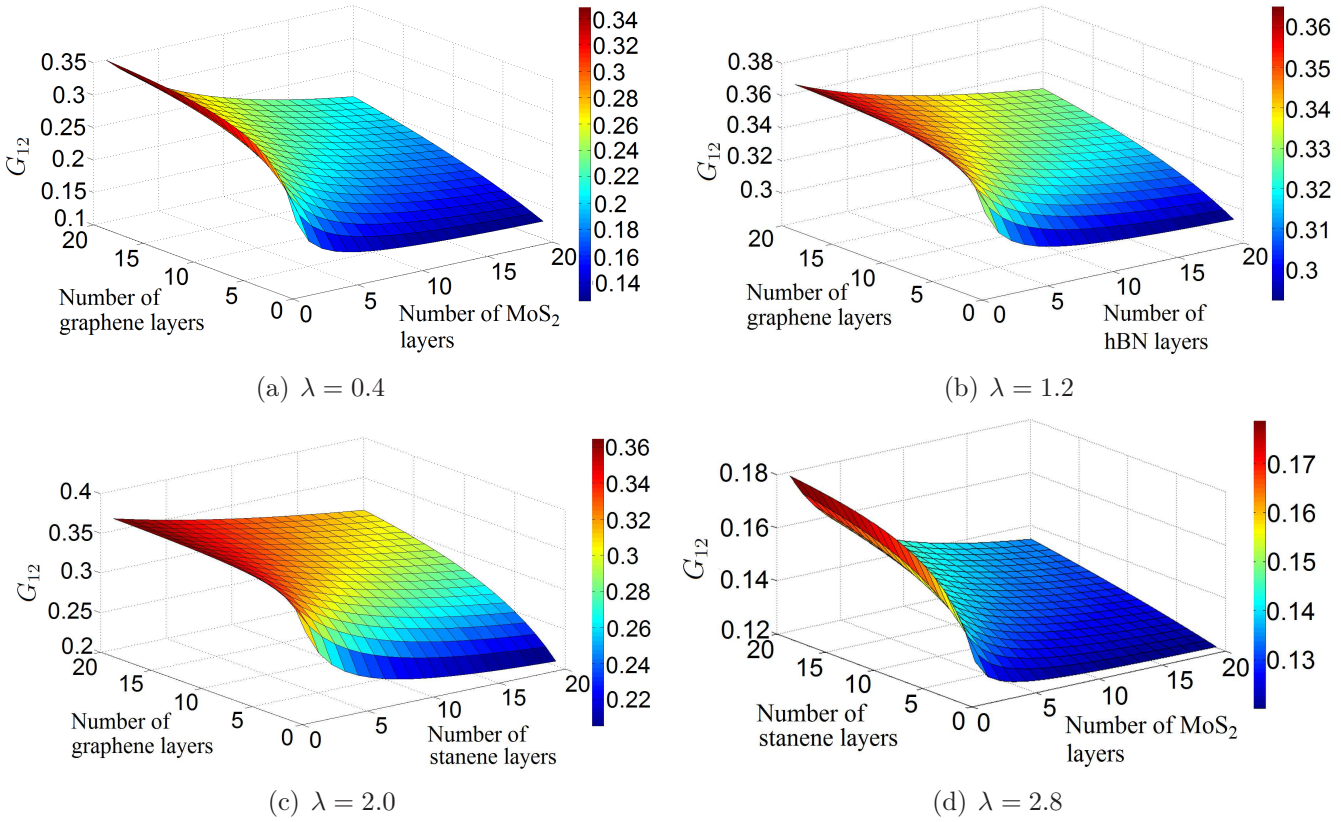

(a) $\lambda = 0.4$ (b) $\lambda = 1.2$

(c) $\lambda = 2.0$ (d) $\lambda = 2.8$

Figure 7: Variation of shear modulus (G_{12}) with number of layers in (a) graphene-MoS_2 heterostructure (b) graphene-hBN heterostructure (c) graphene-stanene heterostructure (d) stanene-MoS_2 heterostructure

shared by the constituent layers depending on their relative individual shear stiffness. However, if other mechanical properties of the heterostructures involving out-of-plane bending characteristics of the heterostructure are investigated, the distance of each layer from the neutral axis would be an important factor. Subsequently the out-of-plane bending characteristics will be stacking-sequence dependent properties. Figure 7 presents the variation of shear modulus with number of layers of the constituent materials considering the four different nano-heterostructures. These plots can readily provide an idea about the nature of variation of shear modulus with stacking sequence for multi-layer nano-heterostructures in a comprehensive manner; exact values of which can be easily obtained using the proposed computationally efficient closed-form formula.

4. Summary and perspective

A major contribution of this article is development of the generalized closed-form formulae for the shear modulus of hexagonal single-layer materials having the atoms in multiple planes (i.e. multiplanar nanostructures such as stanene and MoS_2). Previous literatures have reported the closed-form analytical formulae for Young's moduli and Poisson's ratios of both monoplanar as well as multiplanar single layer nanostructures [32, 42–45]. Recently the analytical expressions for

Young's moduli and Poisson's ratios of nano-heterostructures have been reported [31]. In case of shear modulus, only monoplanar structures have received attention in terms of developing efficient analytical formulae [42, 44], while for multiplanar nanostructural forms, investigations related to shear modulus is very scarce to find even following other approaches such as molecular dynamics simulation, ab initio or laboratory experiments. New results are presented in this article based on the developed analytical approach for such multiplanar nanostructures. The molecular mechanics parameters and structural geometry of different nanomaterials being well-documented in scientific literature, the developed analytical formulae for shear modulus can be applied for wide range of nanostructures. The formulae for hexagonal nanostructures can be readily extended to other forms of nanostructures such as multiplanar square or rectangular forms [98]. Nano-heterostructures being a new field of investigation, results are available only for Young's moduli of graphene-MoS_2 heterostructures based on molecular dynamics simulation. We have presented new results for the shear modulus of four different nano-heterostructures (graphene-MoS_2, graphene-hBN, graphene-stanene and stanene-MoS_2).

Mechanical properties such as Young's moduli, shear modulus and Poisson's ratios are of utmost importance for accessing the viability of a material's use in various applications of nanoelectromechanical systems. Shear modulus assumes a crucial role in determining the resonance frequency of the vibration modes involving torsion, which have been reported to have advantage over the flexural modes for the absence of thermoelastic loss leading to an improvement in mechanical quality factors and device sensitivity parameters. Shear deformation characteristics are also important in the wrinkling and rippling behaviour of two-dimensional materials that control the charge carrier scattering property and electron mobility [33]. The formulae for shear modulus of nanostructures and nano-heterostructures presented in this article can serve as an efficient reference for any nano-scale material having hexagonal structural form. The expressions for obtaining shear modulus of nano-heterostructures are applicable for any stacking sequence of the constituent single layers. Even though results are presented in this article considering only two different constituent materials, the proposed formulae can be used for heterostructures containing any number of different materials [28]. Noteworthy feature of the presented expressions is the computational efficiency and cost-effectiveness compared to performing molecular dynamics simulation or nano-scale experiments. Such development can help to bring about the much-needed impetus in the research of two-dimensional materials, which is often hindered due to the need for carrying out computationally expensive and time consuming simulations/ laboratory experiments and availability of interatomic

potentials. Besides deterministic analysis of shear moduli, as presented in this paper, the efficient closed-form formulae could be an attractive option for carrying out uncertainty analysis [99–104] following a Monte Carlo simulation based approach.

After several years of intensive study, graphene research has logically reached to a rather mature stage. Thus investigation of various other two-dimensional and quasi-two-dimensional materials have started receiving the due attention recently. The possibility of combining single layers of different 2D materials has expanded this field of research dramatically; well beyond the scope of considering a simple single layer graphene or other 2D material. The interest in such heterostructures is growing very rapidly with the advancement of synthesizing such materials in laboratory, as the tremendous amount of research on graphene was observed about a decade ago. The attentiveness is expected to expand further in coming years with the possibility to consider different nanoelectromechanical properties of the prospective combination (single and multi-layer structures with different stacking sequences) of so many 2D materials. This, in turn introduces the possibility of opening a new dimension of application-specific material development (metamaterial) in nano-scale. The efficient closed-form expressions provided in this paper will provide a ready reference for the shear modulus of such heterostructures.

5. Conclusion

Generalized closed-form analytical formulae for the shear modulus of hexagonal multiplanar nano-structures and nano-heterostructures are developed based on a physics-based analytical approach. The dependence of shear modulus on bond length, bond angles and bond strength parameters are explicitly demonstrated. Four different single-layered materials having monoplanar as well as multiplanar structural forms (graphene, hBN, stanene and MoS_2) and four different nano-heterostructures (graphene-MoS_2, graphene-hBN, graphene-stanene and stanene-MoS_2) are considered to present results based on the analytical approach. Good agreement in the results obtained from the derived analytical expressions and results obtained from scientific literature (as available) or separate molecular dynamic simulations corroborates the validity of the proposed formulae. The physics-based analytical formulae are capable of providing a comprehensive in-depth insight regarding the behaviour of multiplanar hexagonal nano-structures and heterostructures under shear deformation. The effect of variation in in-plane and out-of-plane angles to the shear modulus of materials are investigated using the closed-form formulae based on non-dimensional parameters. In case of nano-heterostructures, the variation of shear modulus is presented with number of layers of the constituent materials.

The concept to develop expressions for hexagonal nano-heterostructures can be extended to other forms of nanostrcutures in future. The attractive feature of the developed analytical approach is that it is computationally efficient, physically insightful and easy to implement, yet yields accurate results. As the proposed formulae are general in nature and applicable to wide range of materials and their combinations with hexagonal nano-structures, they can take a crucial role in characterizing the material properties in future nano-materials development.

Acknowledgements

TM acknowledges the financial support from Swansea University through the Zienkiewicz Scholarship. SA acknowledges the financial support from Ser Cymru National Research Network (NRN) with grant no NRN102.

References

[1] Novoselov, K., Geim, A. K., Morozov, S., Jiang, D., Katsnelson, M., Grigorieva, I., Dubonos, S., and Firsov, A. Two-dimensional gas of massless dirac fermions in graphene. *Nature*, 438 (7065):197–200, 2005.

[2] Pan, Y., Zhang, L., Huang, L., Li, L., Meng, L., Gao, M., Huan, Q., Lin, X., Wang, Y., Du, S., et al. Construction of 2d atomic crystals on transition metal surfaces: graphene, silicene, and hafnene. *small*, 10(11):2215–2225, 2014.

[3] Balendhran, S., Walia, S., Nili, H., Sriram, S., and Bhaskaran, M. Elemental analogues of graphene: silicene, germanene, stanene, and phosphorene. *Small*, 11(6):640–652, 2015.

[4] Xu, M., Liang, T., Shi, M., and Chen, H. Graphene–like two–dimensional materials. *Chemical Reviews*, 113(5):3766–3798, 2013.

[5] Das, S., Robinson, J. A., Dubey, M., Terrones, H., and Terrones, M. Beyond graphene: Progress in novel two-dimensional materials and van der waals solids. *Annual Review of Materials Research*, 45:1–27, 2015.

[6] Schwierz, F., Pezoldt, J., and Granzner, R. Two-dimensional materials and their prospects in transistor electronics. *Nanoscale*, 7:8261–8283, 2015.

[7] Chakraborty, P., Das, T., Nafday, D., Boeri, L., and Saha-Dasgupta, T. Manipulating the mechanical properties of ti_2C mxene: Effect of substitutional doping. *Phys. Rev. B*, 95:184106, 2017.

[8] Ghorbani-Asl, M., Borini, S., Kuc, A., and Heine, T. Strain-dependent modulation of conductivity in single-layer transition-metal dichalcogenides. *Phys. Rev. B*, 87:235434, 2013.

[9] Wang, H., Feng, H., and Li, J. Graphene and graphene-like layered transition metal dichalcogenides in energy conversion and storage. *Small*, 10(11):2165–2181, 2014.

[10] Balandin, A. A., Ghosh, S., Bao, W., Calizo, I., Teweldebrhan, D., Miao, F., and Lau, C. N. Superior thermal conductivity of single-layer graphene. *Nano letters*, 8(3):902–907, 2008.

[11] Geim, A. K. and Grigorieva, I. V. Van der waals heterostructures. *Nature*, 499(7459):419–425, 2013.

[12] Zhang, Y. J., Yoshida, M., Suzuki, R., and Iwasa, Y. 2d crystals of transition metal dichalcogenide and their iontronic functionalities. *2D Materials*, 2(4):044004, 2015.

[13] van den Broek, B., Houssa, M., Lu, A., Pourtois, G., Afanas'ev, V., and Stesmans, A. Silicene nanoribbons on transition metal dichalcogenide substrates: Effects on electronic structure and ballistic transport. *Nano Research*, 9(11):3394–3406, 2016.

[14] Houssa, M., van den Broek, B., Iordanidou, K., Lu, A. K. A., Pourtois, G., Locquet, J.-P., Afanas'ev, V., and Stesmans, A. Topological to trivial insulating phase transition in stanene. *Nano Research*, 9(3):774–778, 2016.

[15] Shi, Z. and Singh, C. V. The ideal strength of two-dimensional stanene may reach or exceed the griffith strength estimate. *Nanoscale*, 9:7055–7062, 2017.

[16] Ersan, F., Cahangirov, S., Gökoğlu, G., Rubio, A., and Aktürk, E. Stable monolayer honeycomb-like structures of RuX_2 ($x = S, Se$). *Phys. Rev. B*, 94:155415, 2016.

[17] Li, M.-Y., Chen, C.-H., Shi, Y., and Li, L.-J. Heterostructures based on two-dimensional layered materials and their potential applications. *Materials Today*, 19(6):322 – 335, 2016.

[18] Peng, Q., Hu, K., Sa, B., Zhou, J., Wu, B., Hou, X., and Sun, Z. Unexpected elastic isotropy in a black phosphorene/tic2 van der waals heterostructure with flexible li-ion battery anode applications. *Nano Research*, 10(9):3136–3150, 2017.

[19] Liu, X., Gao, J., Zhang, G., and Zhang, Y.-W. Mos2-graphene in-plane contact for high interfacial thermal conduction. *Nano Research*, 10(9):2944–2953.

[20] Wang, H., Liu, F., Fu, W., Fang, Z., Zhou, W., and Liu, Z. Two-dimensional heterostructures: fabrication, characterization, and application. *Nanoscale*, 6:12250–12272, 2014.

[21] Elder, R. M., Neupane, M. R., and Chantawansri, T. L. Stacking order dependent mechanical properties of graphene/mos2 bilayer and trilayer heterostructures. *Applied Physics Letters*, 107(7):073101, 2015.

[22] Liu, K., Yan, Q., Chen, M., Fan, W., Sun, Y., Suh, J., Fu, D., Lee, S., Zhou, J., Tongay, S., Ji, J., Neaton, J. B., and Wu, J. Elastic properties of chemical-vapor-deposited monolayer

mos2, ws2, and their bilayer heterostructures. *Nano Letters*, 14(9):5097–5103, 2014.

[23] Jiang, J.-W. and Park, H. S. Mechanical properties of mos2/graphene heterostructures. *Applied Physics Letters*, 105(3):033108, 2014.

[24] Zhang, C., Zhao, S., Jin, C., Koh, A. L., Zhou, Y., Xu, W., Li, Q., Xiong, Q., Peng, H., and Liu, Z. Direct growth of large-area graphene and boron nitride heterostructures by a co-segregation method. *Nature communications*, 6, 2015.

[25] Li, Q., Liu, M., Zhang, Y., and Liu, Z. Hexagonal boron nitride–graphene heterostructures: Synthesis and interfacial properties. *Small*, 12(1):32–50, 2016.

[26] Chen, X., Meng, R., Jiang, J., Liang, Q., Yang, Q., Tan, C., Sun, X., Zhang, S., and Ren, T. Electronic structure and optical properties of graphene/stanene heterobilayer. *Physical Chemistry Chemical Physics*, 18(24):16302–16309, 2016.

[27] Ren, C.-C., Feng, Y., Zhang, S.-F., Zhang, C.-W., and Wang, P.-J. The electronic properties of the stanene/mos2 heterostructure under strain. *RSC Adv.*, 7:9176–9181, 2017.

[28] Wang, X. and Xia, F. Van der waals heterostructures: stacked 2d materials shed light. *Nature materials*, 14(3):264–265, 2015.

[29] Entani, S., Antipina, L. Y., Avramov, P. V., Ohtomo, M., Matsumoto, Y., Hirao, N., Shimoyama, I., Naramoto, H., Baba, Y., Sorokin, P. B., and Sakai, S. Contracted interlayer distance in graphene/sapphire heterostructure. *Nano Research*, 8(5):1535–1545, 2015.

[30] Wang, L., Zhou, X., Ma, T., Liu, D., Gao, L., Li, X., Zhang, J., Hu, Y., Wang, H., Dai, Y., and Luo, J. Superlubricity of a graphene/mos2 heterostructure: a combined experimental and dft study. *Nanoscale*, 9:10846–10853, 2017.

[31] Mukhopadhyay, T., Mahata, A., Adhikari, S., and Zaeem, M. A. Effective mechanical properties of multilayer nano-heterostructures. *Scientific Reports*, 7:15818, 2017.

[32] Mukhopadhyay, T., Mahata, A., Adhikari, S., and Zaeem, M. A. Effective elastic properties of two dimensional multiplanar hexagonal nanostructures. *2D Materials*, 4(2):025006, 2017.

[33] Liu, X., Metcalf, T. H., Robinson, J. T., Houston, B. H., and Scarpa, F. Shear modulus of monolayer graphene prepared by chemical vapor deposition. *Nano Letters*, 12(2):1013–1017, 2012.

[34] Zolyomi, V., Wallbank, J. R., and Fal'ko, V. I. Silicane and germanane: tight-binding and first-principles studies. *2D Materials*, 1(1):011005, 2014.

[35] Lorenz, T., Joswig, J.-O., and Seifert, G. Stretching and breaking of monolayer mos2 – an atomistic simulation. *2D Materials*, 1(1):011007, 2014.

[36] Liu, F., Ming, P., and Li, J. Ab initio calculation of ideal strength and phonon instability of graphene under tension. *Physical Review B*, 76(6):064120, 2007.

[37] Debbichi, L., Kim, H., Björkman, T., Eriksson, O., and Lebègue, S. First-principles investigation of two-dimensional trichalcogenide and sesquichalcogenide monolayers. *Phys. Rev. B*, 93:245307, 2016.

[38] Lebègue, S. and Eriksson, O. Electronic structure of two-dimensional crystals from ab initio theory. *Phys. Rev. B*, 79:115409, 2009.

[39] Cherukara, M. J., Narayanan, B., Kinaci, A., Sasikumar, K., Gray, S. K., Chan, M. K., and Sankaranarayanan, S. K. R. S. Ab initio-based bond order potential to investigate low thermal conductivity of stanene nanostructures. *The Journal of Physical Chemistry Letters*, 7(19):3752–3759, 2016.

[40] Grantab, R., Shenoy, V. B., and Ruoff, R. S. Anomalous strength characteristics of tilt grain boundaries in graphene. *Science*, 330(6006):946–948, 2010.

[41] Chang, T. and Gao, H. Size-dependent elastic properties of a single-walled carbon nanotube via a molecular mechanics model. *Journal of the Mechanics and Physics of Solids*, 51(6): 1059–1074, 2003.

[42] Scarpa, F., Adhikari, S., and Phani, A. S. Effective elastic mechanical properties of single layer graphene sheets. *Nanotechnology*, 20(6):065709, 2009.

[43] Shokrieh, M. M. and Rafiee, R. Prediction of young's modulus of graphene sheets and carbon nanotubes using nanoscale continuum mechanics approach. *Materials & Design*, 31:790–795, 2010.

[44] Boldrin, L., Scarpa, F., Chowdhury, R., and Adhikari, S. Effective mechanical properties of hexagonal boron nitride nanosheets. *Nanotechnology*, 22(50):505702, 2011.

[45] Le, M.-Q. Prediction of young's modulus of hexagonal monolayer sheets based on molecular mechanics. *International Journal of Mechanics and Materials in Design*, 11(1):15–24, 2015.

[46] Li, Y., Zhang, W., Guo, B., and Datta, D. Interlayer shear of nanomaterials: Graphene–graphene, boron nitride–boron nitride and graphene–boron nitride. *Acta Mechanica Solida Sinica*, 30(3):234 –240, 2017.

[47] Gelin, B. R. *Molecular Modeling of Polymer Structures and Properties*. Hanser Gardner Publications, 1994.

[48] Zhang, J. and Wang, C. Free vibration analysis of microtubules based on the molecular mechanics and continuum beam theory. *Biomechanics and Modeling in Mechanobiology*, 15

(5):1069–1078, 2016.

[49] Gibson, L. and Ashby, M. F. *Cellular Solids Structure and Properties*. Cambridge University Press, Cambridge, UK, 1999.

[50] Mukhopadhyay, T. and Adhikari, S. Equivalent in-plane elastic properties of irregular honeycombs: An analytical approach. *International Journal of Solids and Structures*, 91:169 – 184, 2016.

[51] Mukhopadhyay, T. and Adhikari, S. Effective in-plane elastic properties of auxetic honeycombs with spatial irregularity. *Mechanics of Materials*, 95:204 – 222, 2016.

[52] Mukhopadhyay, T. and Adhikari, S. Free vibration analysis of sandwich panels with randomly irregular honeycomb core. *Journal of Engineering Mechanics*, 10.1061/(ASCE)EM.1943-7889.0001153 , 06016008, 2016.

[53] Mukhopadhyay, T. and Adhikari, S. Stochastic mechanics of metamaterials. *Composite Structures*, 2016. doi: http://dx.doi.org/10.1016/j.compstruct.2016.11.080.

[54] Mukhopadhyay, T., Adhikari, S., and Batou, A. Frequency domain homogenization for the viscoelastic properties of spatially correlated quasi-periodic lattices. *International Journal of Mechanical Sciences*, 2017. doi: https://doi.org/10.1016/j.ijmecsci.2017.09.004.

[55] Mukhopadhyay, T. and Adhikari, S. Effective in-plane elastic moduli of quasi-random spatially irregular hexagonal lattices. *International Journal of Engineering Science*, 119:142 – 179, 2017.

[56] Huang, C., Chen, C., Zhang, M., Lin, L., Ye, X., Lin, S., Antonietti, M., and Wang, X. Carbon-doped bn nanosheets for metal-free photoredox catalysis. *Nature communications*, 6, 7698, 2015.

[57] Zhu, F., Chen, W., Xu, Y., Gao, C., Guan, D., Liu, C., Qian, D., Zhang, S., and Jia, J. Epitaxial growth of two-dimensional stanene. *Nature materials*, 14(10):1020–1025, 2015.

[58] Ni, Z., Liu, Q., Tang, K., Zheng, J., Zhou, J., Qin, R., Gao, Z., Yu, D., and Lu, J. Tunable bandgap in silicene and germanene. *Nano Letters*, 12(1):113–118, 2012.

[59] Liu, H., Neal, A. T., Zhu, Z., Luo, Z., Xu, X., Tomanek, D., and Ye, P. D. Phosphorene: An unexplored 2d semiconductor with a high hole mobility. *ACS Nano*, 8(4):4033–4041, 2014.

[60] Mannix, A. J., Zhou, X., Kiraly, B., Wood, J. D., Alducin, D., Myers, B. D., Liu, X., Fisher, B. L., Santiago, U., Guest, J. R., Yacaman, M. J., Ponce, A., Oganov, A. R., Hersam, M. C., and Guisinger, N. P. Synthesis of borophenes: Anisotropic, two-dimensional boron polymorphs. *Science*, 350(6267):1513–1516, 2015.

[61] Brunier, T. M., Drew, M. G. B., and Mitchell, P. C. H. Molecular mechanics studies of

molybdenum disulphide catalysts parameterisation of molybdenum and sulphur. *Molecular Simulation*, 9(2):143–159, 1992.

[62] Cooper, R. C., Lee, C., Marianetti, C. A., Wei, X., Hone, J., and Kysar, J. W. Nonlinear elastic behavior of two-dimensional molybdenum disulfide. *Phys. Rev. B*, 87:035423, 2013.

[63] Balendhran, S., Ou, J. Z., Bhaskaran, M., Sriram, S., Ippolito, S., Vasic, Z., Kats, E., Bhargava, S., Zhuiykov, S., and Kalantar-zadeh, K. Atomically thin layers of mos2 via a two step thermal evaporation-exfoliation method. *Nanoscale*, 4:461–466, 2012.

[64] Zhao, W., Ghorannevis, Z., Chu, L., Toh, M., Kloc, C., Tan, P.-H., and Eda, G. Evolution of electronic structure in atomically thin sheets of ws2 and wse2. *ACS Nano*, 7(1):791–797, 2013.

[65] Coehoorn, R., Haas, C., Dijkstra, J., Flipse, C. J. F., de Groot, R. A., and Wold, A. Electronic structure of $mose_2$, mos_2, and wse_2. i. band-structure calculations and photoelectron spectroscopy. *Physical review B*, 35:6195–6202, 1987.

[66] Ruppert, C., Aslan, O. B., and Heinz, T. F. Optical properties and band gap of single- and few-layer mote2 crystals. *Nano Letters*, 14(11):6231–6236, 2014.

[67] Bruzzone, S., Logoteta, D., Fiori, G., and Iannaccone, G. Vertical transport in graphene-hexagonal boron nitride heterostructure devices. *Scientific reports*, 5, 2015.

[68] Cai, Y., Zhang, G., and Zhang, Y.-W. Electronic properties of phosphorene/graphene and phosphorene/hexagonal boron nitride heterostructures. *The Journal of Physical Chemistry C*, 119(24):13929–13936, 2015.

[69] Li, C. and Chou, T. W. A structural mechanics approach for the analysis of carbon nanotubes. *International Journal of Solids and Structures*, 40(10):2487 – 2499, 2003.

[70] Cornell, W. D., Cieplak, P., Bayly, C. I., Gould, I. R., Merz, K. M., Ferguson, D. M., Spellmeyer, D. C., Fox, T., Caldwell, J. W., and Kollman, P. A. A second generation force field for the simulation of proteins, nucleic acids, and organic molecules. *Journal of the American Chemical Society*, 117(19):5179–5197, 1995.

[71] Mayo, S. L., Olafson, B. D., and Goddard, W. A. Dreiding: a generic force field for molecular simulations. *The Journal of Physical Chemistry*, 94(26):8897–8909, 1990.

[72] Li, C. and Chou, T.-W. Static and dynamic properties of single-walled boron nitride nanotubes. *Journal of nanoscience and nanotechnology*, 6(1):54–60, 2006.

[73] Modarresi, M., Kakoee, A., Mogulkoc, Y., and Roknabadi, M. Effect of external strain on electronic structure of stanene. *Computational Materials Science*, 101:164 – 167, 2015.

[74] Wang, D., Chen, L., Wang, X., Cui, G., and Zhang, P. The effect of substrate and external strain on electronic structures of stanene film. *Phys. Chem. Chem. Phys.*, 17:26979–26987, 2015.

[75] Tang, P., Chen, P., Cao, W., Huang, H., Cahangirov, S., Xian, L., Xu, Y., Zhang, S.-C., Duan, W., and Rubio, A. Stable two-dimensional dumbbell stanene: A quantum spin hall insulator. *Phys. Rev. B*, 90:121408, 2014.

[76] van den Broek, B., Houssa, M., Scalise, E., Pourtois, G., Afanasev, V. V., and Stesmans, A. Two-dimensional hexagonal tin: ab initio geometry, stability, electronic structure and functionalization. *2D Materials*, 1(2):021004, 2014.

[77] Bronsema, K., De Boer, J., and Jellinek, F. On the structure of molybdenum diselenide and disulfide. *Zeitschrift für anorganische und allgemeine Chemie*, 540(9-10):15–17, 1986.

[78] Wieting, T. and Verble, J. Infrared and raman studies of long-wavelength optical phonons in hexagonal mos2. *Physical Review B*, 3(12):4286, 1971.

[79] Ma, Z. and Dai, S. Ab initio studies on the electronic structure of the complexes containing mo–s bond using relativistic effective core potentials. *Acta Chimica Sinica English Edition*, 7 (3):201–208, 1989.

[80] Sakhaee-Pour, A. Elastic properties of single layered graphene sheet. *Solid State Communications*, 149:91–95, 2009.

[81] Zakharchenko, K. V., Katsnelson, M. I., and Fasolino, A. Finite temperature lattice properties of graphene beyond the quasiharmonic approximation. *Phys. Rev. Lett.*, 102:046808, Jan 2009.

[82] Jiang, L. and Guo, W. A molecular mechanics study on size-dependent elastic properties of single-walled boron nitride nanotubes. *Journal of the Mechanics and Physics of Solids*, 59(6): 1204 – 1213, 2011.

[83] Bosak, A., Serrano, J., Krisch, M., Watanabe, K., Taniguchi, T., and Kanda, H. Elasticity of hexagonal boron nitride: Inelastic x-ray scattering measurements. *Phys. Rev. B*, 73:041402, 2006.

[84] Verma, V., Jindal, V. K., and Dharamvir, K. Elastic moduli of a boron nitride nanotube. *Nanotechnology*, 18(43):435711, 2007.

[85] Plimpton, S. Fast parallel algorithms for short-range molecular dynamics. *Journal of computational physics*, 117(1):1–19, 1995.

[86] Brenner, D. W., Shenderova, O. A., Harrison, J. A., Stuart, S. J., Ni, B., and Sinnott, S. B. A second-generation reactive empirical bond order (rebo) potential energy expression

for hydrocarbons. *Journal of Physics: Condensed Matter*, 14(4):783, 2002.

[87] Liang, T., Phillpot, S. R., and Sinnott, S. B. Parametrization of a reactive many-body potential for mo–s systems. *Physical Review B*, 79(24):245110, 2009.

[88] Shenderova, O., Brenner, D., Omeltchenko, A., Su, X., and Yang, L. Atomistic modeling of the fracture of polycrystalline diamond. *Physical Review B*, 61(6):3877, 2000.

[89] Zhao, H., Min, K., and Aluru, N. Size and chirality dependent elastic properties of graphene nanoribbons under uniaxial tension. *Nano letters*, 9(8):3012–3015, 2009.

[90] Jiang, J.-W., Wang, J.-S., and Li, B. Young's modulus of graphene: a molecular dynamics study. *Physical Review B*, 80(11):113405, 2009.

[91] Xiao, J., Staniszewski, J., and Gillespie, J. Fracture and progressive failure of defective graphene sheets and carbon nanotubes. *Composite structures*, 88(4):602–609, 2009.

[92] Stewart, J. A. and Spearot, D. Atomistic simulations of nanoindentation on the basal plane of crystalline molybdenum disulfide (mos2). *Modelling and Simulation in Materials Science and Engineering*, 21(4):045003, 2013.

[93] Li, M., Wan, Y., Tu, L., Yang, Y., and Lou, J. The effect of v mos3 point defect on the elastic properties of monolayer mos2 with rebo potentials. *Nanoscale research letters*, 11(1): 155, 2016.

[94] Chen, C.-C., Li, Z., Shi, L., and Cronin, S. B. Thermoelectric transport across graphene/hexagonal boron nitride/graphene heterostructures. *Nano Research*, 8(2):666–672, 2015.

[95] Neek-Amal, M. and Peeters, F. Nanoindentation of a circular sheet of bilayer graphene. *Physical Review B*, 81(23):235421, 2010.

[96] Jiang, J.-W. and Park, H. S. Mechanical properties of mos2/graphene heterostructures. *Applied Physics Letters*, 105(3):033108, 2014.

[97] Elder, R. M., Neupane, M. R., and Chantawansri, T. L. Stacking order dependent mechanical properties of graphene/mos2 bilayer and trilayer heterostructures. *Applied Physics Letters*, 107(7):073101, 2015.

[98] Sorkin, V. and Zhang, Y. W. The structure and elastic properties of phosphorene edges. *Nanotechnology*, 26(23):235707, 2015.

[99] Mukhopadhyay, T., Mahata, T., Dey, S., and Adhikari, S. Probabilistic analysis and design of hcp nanowires: An efficient surrogate based molecular dynamics simulation approach. *Journal of Materials Science & Technology*, 32(12):1345 – 1351, 2016.

[100] Mahata, A., Mukhopadhyay, T., and Adhikari, S. A polynomial chaos expansion based molecular dynamics study for probabilistic strength analysis of nano-twinned copper. *Materials Research Express*, 3(3):036501, 2016.

[101] Naskar, S., Mukhopadhyay, T., Sriramula, S., and Adhikari, S. Stochastic natural frequency analysis of damaged thin-walled laminated composite beams with uncertainty in micromechanical properties. *Composite Structures*, 160:312 – 334, 2017.

[102] Dey, S., Mukhopadhyay, T., Naskar, S., Dey, T., Chalak, H., and Adhikari, S. Probabilistic characterisation for dynamics and stability of laminated soft core sandwich plates. *Journal of Sandwich Structures & Materials*. doi: 10.1177/1099636217694229.

[103] Dey, S., Mukhopadhyay, T., Sahu, S., and Adhikari, S. Stochastic dynamic stability analysis of composite curved panels subjected to non-uniform partial edge loading. *European Journal of Mechanics - A/Solids*, 67:108 – 122, 2018.

[104] Dey, S., Mukhopadhyay, T., Sahu, S., and Adhikari, S. Effect of cutout on stochastic natural frequency of composite curved panels. *Composites Part B: Engineering*, 105:188 – 202, 2016.